ANNALS OF GEOPHYSICS, VOL. 47, N. 1, February 2004

Robust satellite techniques for volcanic and seismic hazards monitoring

Gerardo Di Bello ([1]), **Carolina Filizzola** ([1]), **Teodosio Lacava** ([1]), **Francesco Marchese** ([2]), **Nicola Pergola** ([3]), **Carla Pietrapertosa** ([3]), **Sabatino Piscitelli** ([3]), **Irene Scaffidi** ([3]) **and Valerio Tramutoli** ([1])

([1]) *Dipartimento di Ingegneria e Fisica dell'Ambiente, Università degli Studi della Basilicata, Potenza, Italy*

([2]) *Dipartimento di Scienze Geologiche, Università degli Studi della Basilicata, Potenza, Italy*

([3]) *Istituto di Metodologie per l'Analisi Ambientale (IMAA),CNR, Tito Scalo (PZ), Italy*

Abstract

Several satellite techniques have been proposed to monitor events related to seismic and volcanic activity. A self-adaptive approach (RAT, Robust AVHRR Techniques) has recently been proposed which seems able to recognise space-time anomalies, differently related to such events, also in the presence of highly variable contributions from atmospheric (transmittance), surface (emissivity and morphology) and observational (time/season, but also solar and satellite zenithal angles) conditions. On the basis of NOAA-AVHRR data, the RAT aprroach has already been applied to Mount Etna volcanic ash cloud monitoring in daytime, and to seismic area monitoring in Southern Italy. This paper presents the theoretical basis for the extension of RAT approach also to nighttime volcanic ash cloud detection, together with its possible implementation to lava flow monitoring. One example of successful forecasting (few days before) of a new lava vent opening during the Mount Etna eruption of July 2001 will be discussed in some detail. Progress on the use of the same approach on seismically active area monitoring will be discussed by comparison with previous results achieved on the Irpinia-Basilicata earthquake (M_S = 6.9), which occurred on November 23rd 1980 in Southern Italy.

Key words *lava flows – volcanic ash clouds – Irpinia-Basilicata earthquake – Robust AVHRR Techniques – TIR anomaly*

1. Introduction

Several satellite techniques have been proposed to monitor seismic and volcanic activity and to possibly mitigate related hazards.

As far as an early warning and real-time monitoring of volcano activity are concerned, satellites with shorter revisiting times have usually been preferred despite their relatively coarse spatial resolution. For applications like volcanic ash-cloud detection and tracking, spatial resolutions of a few kilometres (faced with revisiting times of 30 min and less), offered by geo-stationary satellites (like GOES, GMS, etc.), were sufficient to implement operational satellite-based systems (like VAACs, Volcanic Ash Advisory Centres), devoted to worldwide support flight safety. On the other hand, due to the high radiant temperature involved, even the spatial resolution of 1.1 km (nadir-view) offered by sounders like AVHRR (Advanced Very High Resolution Radiometer, on board NOAA, US National Oceanic and Atmospheric Administration, satellites) has proved useful since 1964 (*e.g.*, Gawarecky *et al.,* 1965) for volcanic lava flow detection and monitoring. Even if other satellite sounders, with higher spatial and/or

Mailing address: Dr. Valerio Tramutoli, Dipartimento di Ingegneria e Fisica dell'Ambiente, Università degli Studi della Basilicata, Via dell'Ateneo Lucano 10, 85100 Potenza, Italy; e-mail: Tramutoli@unibas.it

spectral capabilities are now available for studying volcanic activity (from the historical LANDSAT Thematic Mapper up to the more recent MODIS and ASTER sensors on the EOS platforms), time resolution (from few days to few weeks) and present data policy (data access and/or costs) still represent the main obstacles for an extended use of such sensors for real-time monitoring of volcanoes (Carn and Oppenheimer, 2000). After 20 years of activity (scheduled to continue at least up to 2010), AVHRR is still one of the best instruments for real-time volcano activity monitoring. The most quoted AVHRR techniques for volcanic activity monitoring are those first proposed by Prata (1989) for volcanic ash monitoring, and by Harris and Swabey (1995) for active lava detection. Both techniques, subsequently amended and/or improved by the same and by other authors, make use of a fixed threshold approach. For example, in the case of Prata's split window method, volcanic ash clouds are identified (discriminating them from meteorological clouds) in correspondence with AVHRR pixels having $T_4 - T_5 < 0$ K (T_4 and T_5 being the radiances, expressed in brightness temperature, measured, respectively, in the thermal infrared AVHRR channel 4 and 5). Similarly, AVHRR pixels containing active lava are identified (discriminating them from high reflective and/or hot exposed rocks) by the Harris and Swabey method, in correspondence with AVHRR pixels having $T_3 + - T_4 > 10$ K (T_3 being the radiance, expressed in brightness temperature, measured in the medium infrared AVHRR channel 3). As we will see, both techniques, even if effective in most cases, also give false or missing identification under particular (but not rare) observational conditions, and for specific atmospheric and Earth surface features.

The relatively low spatial resolution of AVHRR has not been considered a barrier even for studies on seismic activity. Since the pioneer study of Gorny *et al.* (1988), several authors have reported large scale outbreaks (extending for hundreds of kilometres) of TIR (thermal infrared) anomalies in some relation with time and place of occurrence of severe earthquakes in China (Qiang and Chang-Gong, 1992; Qiang *et al.*, 1997), Central Asia (Tronin, 1996), and Japan (Tronin *et al.*, 2002). Some rash conclusions and claimed results of similar studies have been considered with prudence by the scientific community, mainly due to the insufficiency of the validation data-sets and the scarce importance attached by authors to other causes (*e.g.*, meteorological) that, rather than seismic activity, could cause the observed TIR anomalies.

Also in this case, anomalous transients in the observed satellite signal are evaluated in absolute terms and not by reference to a normal signal behaviour that, as experience teaches, is specific for time and place (*llocal*, as defined in Tramutoli, 1998) of observations. In fact, the same signal, which is normally observable at a specific time and place, could prove anomalous when observed in a different time and place. Using a fixed threshold approach, for whatever place and time, imposes a choice between reliability (that would require more drastic thresholds) and sensitivity (low level thresholds) that, due to the normal space-time variability of the signal, produces missing (in the first case) or false (in the second case) detection proliferation.

This paper will deal with the problem of resolving, in space-time signal transients, such a natural/observational noise, whose variable contribution to satellite radiances (signal) can be so high as to completely hide (missing detections) or simulate (false detections) signal transients possibly associated with the events under study.

This problem has already been successfully tackled by applying the RAT (Robust AVHRR Techniques) approach (Tramutoli, 1998) to the detection and monitoring of wildfires (Cuomo, *et al.*, 2001) and meteorological (Pietrapertosa *et al.*, 2001) and volcanic (Pergola *et al.*, 2001; Tramutoli *et al.*, 2001a) clouds using AVHRR VIS (visible), NIR (near-infrared) and MIR (mid-infrared) radiances. On the basis of NOAA-AVHRR data, RAT has already been applied to Mount Etna volcanic ash cloud monitoring in daytime (Pergola *et al.*, 2001) as well as seismic area monitoring in Southern Italy (Tramutoli *et al.*, 2001b). The RAT approach permitted us to recognise space-time anomalies, related differently to such events, also in the presence of highly variable contributions

from atmospheric (transmittance), surface (emissivity and morphology) and observational (time/season, but also solar and satellite view angles) conditions. To accomplish this, RAT exploits all the information contained in long-term series of satellite records $\{V(x, y, t), t \in T\}$, collected under similar observational conditions at location (x, y) in order to characterize the signal behaviour in terms of expected value $V_{\mathrm{REF}}(x, y)$ and variability $\sigma_V(x, y)$ in unperturbed conditions to be analysed by comparison with the signal $V(x, y, t)$ at hand. An anomalous space-time transient is then evaluated on the basis of the history of the signal at the site (x, y), by an index like ALICE (Absolutely Local Index of Change of the Environment, Tramutoli, 1998)

$$\otimes_V(x, y, t) = \frac{V(x, y, t) - V_{\mathrm{REF}}(x, y)}{\sigma_V(x, y)} \qquad (1.1)$$

which provides at the pixel-level an estimate of the difference between the signal $V(x, y, t)$ observed at time t and its expected value $V_{\mathrm{REF}} \cdot \cdot(x, y)$, weighted by the historically observed signal variability $\sigma_V(x, y)$ which includes all the possible noise sources not related to the event to be monitored. The robustness of this approach is intrinsic, because the higher the variability $\sigma_V(x, y)$ of the signal (in the chosen temporal domain T) is, the harder it will be to achieve high values of $\otimes_V(x, y, t)$, reducing, in this way, the problem of false alarms. It should be stressed that such an approach, being exclusively based on satellite data, (without any other ancillary information), is fully exportable on which ever satellite/sensor system and in whatever geographic area.

In this paper, the theoretical basis for the extension of RAT approach also to night-time volcanic ash cloud detection will be presented together with its possible implementation to lava flow monitoring. One example of successful forecasting (a few days before) of a new lava vent opening during the Mount Etna eruption of July 2001 will be discussed in some detail.

Progress on the use of the same approach on seismically active area monitoring will be discussed by comparison with previous results achieved on the Irpinia-Basilicata earthquake ($M_S = 6.9$) which occurred on November 23rd 1980 in Southern Italy.

2. Volcanic ash cloud monitoring

As mentioned before, the volcanic ash detection method suggested first by Prata (1989), has been widely used in the last decade and further improved by the scientific community (*e.g.*, Holasek and Rose, 1991; Schneider and Rose, 1994, 1995; Rose and Schneider, 1996; Davies and Rose, 1998; Ellrod and Connell, 1999). It uses the difference of brightness temperatures measured by satellite sensors (like AVHRR) in two contiguous infrared spectral channels («split-window»), around 11 μm (hereafter T_4) and 12 μm (hereafter T_5). Due to the spectral properties of semi-transparent volcanic clouds (mainly due to acid components and ash particles), eruptive volcanic plumes are expected to give negative ($T_4 - T_5$) differences, whereas semi-transparent meteorological clouds should generally lead to positive values. Even if the usefulness of such a technique in discriminating volcanic clouds from water/ice clouds has been confirmed by several studies (*e.g.*, Schneider and Rose, 1994, 1995; Davies and Rose, 1998), its reliability has been demonstrated not to be satisfactory in several circumstances. In fact, a high concentrations of water vapour in the atmosphere, or contained inside the eruptive plume (quite common in the first few hours following the eruption) can compensate the expected reverse absorption effect giving positive ($T_4 - T_5$) differences which prevent the above mentioned method from correctly identifying ash clouds (Wen and Rose, 1994; Krotkov *et al.,* 1999; Simpson *et al.,* 2000). Wen and Rose (1994) recognise that such a reverse effect completely disappears for particle size greater than 5 μm as well as for totally opaque clouds. A similar problem arises in the presence of a cold surface background, not so rare, especially during the winter, due to the low contrast between TIR radiances coming from the ash cloud and the underlying surface (Wen and Rose, 1994; Rose and Schneider, 1996; Seftor *et al.,* 1997; Pergola *et al.,* 2001).

As an example, figs. 1a,b and 2a-c show two cases of eruptive plumes at Mount Etna on July 23rd 2001 at 12:00 GMT and on July 30th 2001 at 01:00 GMT that result poorly detected or completely missed using the simple $\Delta T_{4-5} = T_4 + - T_5 < 0$ K Prata's test. The reason is quite clear looking at the behaviour of ΔT_{4-5} signal across the volcanic plume (figs. 1b and 2b). Even if

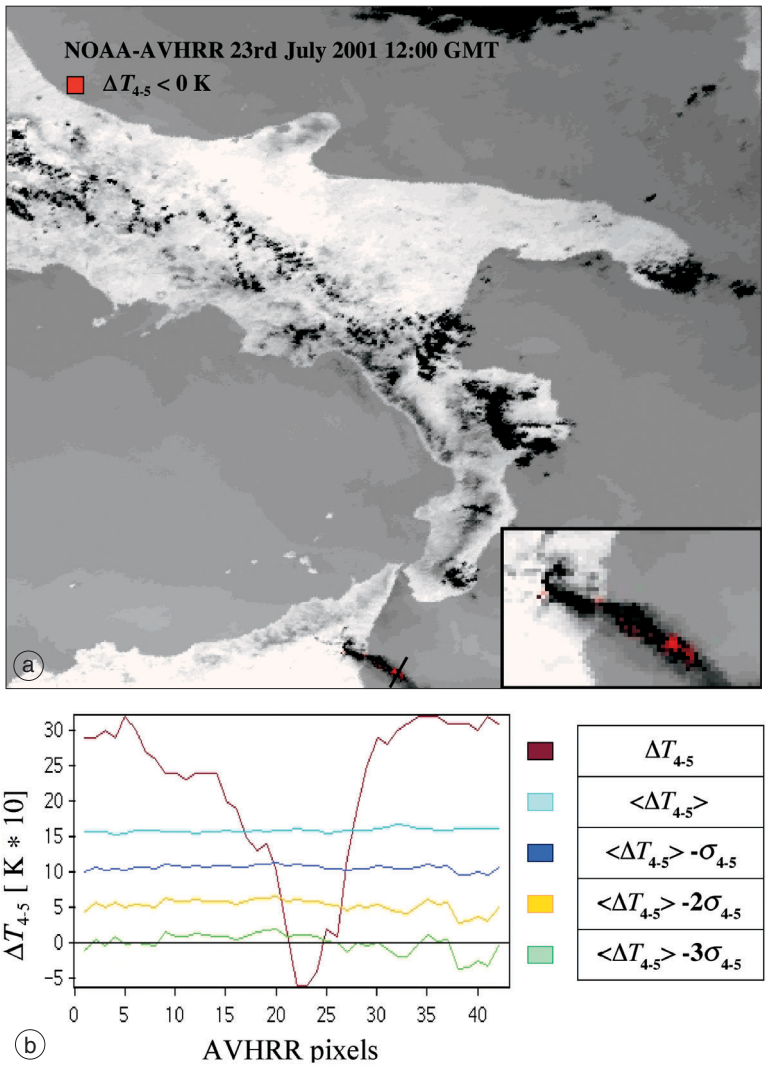

Fig. 1a,b. NOAA/AVHRR July 23rd 2001, 12:00 GMT: a) pixels satisfying Prata's test, $\Delta T_{4-5} < 0$ (see text), are depicted in red; in background AVHRR channel 4 brightness temperatures are depicted in grey tones (light tones correspond to higher BT values). Details of the eruptive plume are given in the box. b) The behaviour of ΔT_{4-5} signal across the transect drawn in (a) is plotted together with its reference values corresponding to $\otimes_{4-5}(x, y, t)$ cuts at values in between 0 (*i.e.* $\Delta T_{4-5} = \langle \Delta T_{4-5} \rangle$) and – 3 (*i.e.* $\Delta T_{4-5} = \langle \Delta T_{4-5} \rangle - 3\,\sigma_{4-5}$). Note how most of the ash plume exhibits positive ΔT_{4-5} values undetectable by Prata's fixed threshold test but still recognizable by RAT approach (see text).

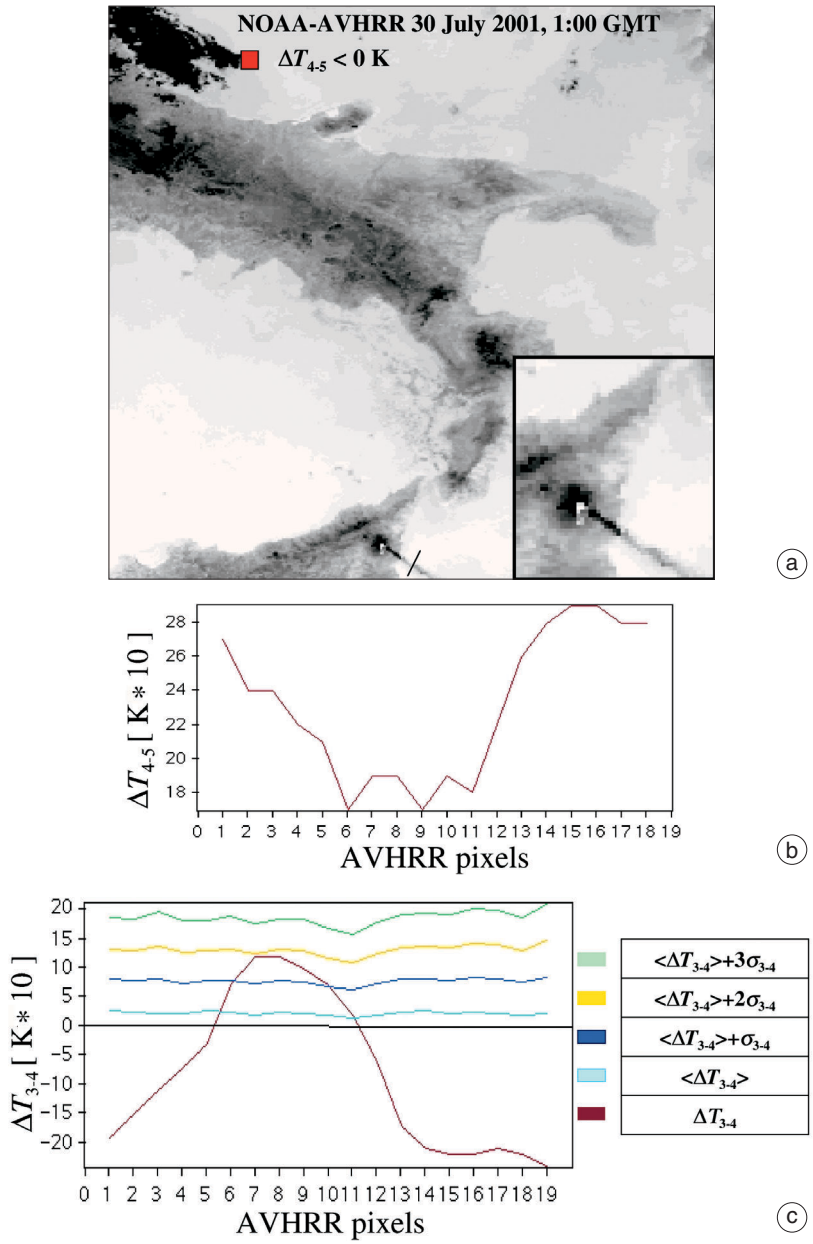

Fig. 2a-c. NOAA/AVHRR July 30th 2001, 1:00 GMT: a) as in fig. 1a; b) plots of ΔT_{4-5} signal across the transect drawn in (a): note as ash plume exhibits only positive ΔT_{4-5} values being completely undetected by Prata's fixed threshold test; c) ΔT_{3-4} signal (see text) is plotted together with its reference values corresponding to $\otimes_{3-4}(x, y, t)$ cuts at values in between 0 (*i.e.* $\Delta T_{3-4} = \langle \Delta T_{3-4} \rangle$) and 3 (*i.e.* $\Delta T_{3-4} = \langle \Delta T_{3-4} \rangle + 3\ \sigma_{3-4}$). Note how the presence of the ash plume is detectable by RAT approach also on the basis of $\otimes_{3-4}(x, y, t)$ index (see text).

ΔT_{4-5} is, on the plume, clearly smaller than on the neighbouring surface background, only for a few pixels on 23rd July (never in the 30th July case) does its value reach the negative level required by Prata's test to make the volcanic plume detectable.

In these cases, the RAT approach could provide a statistics-based method to dynamically define the discrimination thresholds, without having recourse to any other information except for satellite records. Starting from the general expression (1.1) and considering the variable $V \cdot (x, y, t) = [T_4 (x, y, t) - T_5 (x, y, t)] \equiv \Delta T_{4-5} (x, y, t)$ the ALICE index can be defined as

$$\otimes_{\Delta T_{4-5}} (x, y, t) = \frac{\Delta T_{4-5}(x, y, t) - \langle \Delta T_{4-5}(x, y) \rangle}{\sigma_{\Delta T_{4-5}}(x, y)} \tag{2.1}$$

where the quantities $\langle \Delta T_{4-5} (x, y) \rangle$ and $\sigma_{\Delta T} (x, y)$ are, respectively, the mean values and the standard deviations of quantity $\Delta T_{4-5} (x, y, t)$ computed over a long-term series of unperturbed satellite records, collected in similar observational conditions. The first one represents the background signal observed in unperturbed conditions, whereas the second one takes account of the natural variability of the signal in the series. Following RAT prescriptions on data set homogeneity (for details see: Tramutoli, 1998), in the cases of figs. 1a,b and 2a-c, the reference images $\langle \Delta T_{4-5} (x, y) \rangle$ and $\sigma_{4-5} (x, y)$ were computed on the basis of co-located, cloud-free, AVHRR records collected during the month of July in the years from 1996 to 2001. Only AVHRR images collected around 12:00 GMT were used to build the reference images for the 23rd July case, and only the ones collected around midnight for the 30th July case. In fig. 1b, for the 23rd July case, the behaviour of index $\otimes_{4-5} (x, y, t)$ is represented (along the same transects across the ash plume) for values in between 0 (*i.e.* $\Delta T_{4-5} = \langle \Delta T_{4-5} \rangle$) and – 3 (*i.e.* $\Delta T_{4-5} = \langle \Delta T_{4-5} \rangle - 3\sigma_{4-5}$). It is quite evident that most of the ash plume also exhibits positive ΔT_{4-5} values (up to 2.5 K) and that the use of *llocal* thresholds (already at $\otimes_{4-5} (x, y, t) < -1$) could permit a better description of the actual ash plume extension.

Recently, other authors have proposed different detection schemes which make use of MIR (medium infrared around 3.5 μm, hereafter T_3) radiances suggesting the $T_3 - T_4$ difference as a further indicator of ash clouds (Ellrod and Connell, 1999). Also in these cases, major problems arise with the use of a «fixed threshold» approach that affects the reliability of such methods under particular observational conditions (*e.g.,* night/day, thin cirrus clouds, etc.; Scaffidi, 2001). Also in this case the RAT approach could permit us to dynamically define suitable discrimination thresholds automatically computed, not *a priori*, but only on the basis of satellite records. In this case the general expression (1.1) applied to the variable $V (x, y, t) = [T_3 (x, y, t) - T_4 (x, y, t)] \equiv \Delta T_{3-4} (x, y, t)$ permits us to define the ALICE index

$$\otimes_{\Delta T_{3-4}} (x, y, t) = \frac{\Delta T_{3-4}(x, y, t) - \langle \Delta T_{3-4}(x, y) \rangle}{\sigma_{\Delta T_{3-4}}(x, y)} \tag{2.2}$$

where, the quantities $\langle \Delta T (x, y) \rangle$ and $\sigma_{3-4} (x, y)$ have the same meaning and play the same role as described for expression (2.2). In fig. 2c, for the 30th July case, the behaviour of the index $\otimes_{3-4} (x, y, t)$ (along the same transects across the ash plume) for values in between 0 (*i.e.* $\Delta T_{3-4} = \langle \Delta T_{3-4} \rangle$) and 3 (*i.e.* $\Delta T_{3-4} = \langle \Delta T_{3-4} \rangle + 3\ \sigma_{3-4}$) is represented. It is quite evident that most of the ash plume also exhibits negative ΔT_{3-4} values (up to – 2 K) and that the use of *llocal* thresholds (already at $\otimes_{3-4} (x, y, t) > 1$) could permit us a better description of ash plume extension also by using the $T_3 - T_4$ indicator. Preliminary tests (Scaffidi, 2001) performed on several Mount Etna eruptive events show that the combined use of indices (2.1) and (2.2) strongly reduces false and missing volcanic ash identification, also in those cases where traditional, fixed threshold approaches, fail.

3. Active lava flow monitoring

Satellite remote sensing of hot-spots (like molten lava or gas emission of high temperature) mainly relies on the high temperature contrast

with the adjacent (colder) surfaces that, at nighttime, can be better appreciated in the MIR atmospheric window around 3.5 μm. However, in daytime, within that spectral region, the solar radiation reflected by exposed soils, and the natural warming of volcanic rocks, can be responsible for a signal at the sensor as high as to exceed the dynamic range of MIR detectors. In these cases, a simple threshold approach on satellite MIR radiances, would generate false identification (Oppenheimer, 1998). To solve such a problem, Harris and Swabey (1995) proposed a two-channel method based on the difference between brightness temperatures measured in AVHRR channel 3 (at 3.55-3.94 μm, hereafter T_3) and channel 4 (10.3-11.3 μm, hereafter T_4). Since channel 3 is more sensitive than channel 4 to hot sources at magmatic temperatures, whereas both should be equally sensitive to solar heated surfaces, volcanic hot-spots may be detected at higher $\Delta T_{3-4} = (T_3 - T_4)$ values. Also in this case a fixed threshold test ($\Delta T_{3-4} > 10$ K) was proposed. Higgins and Harris (1997), in order to detect thermal anomalies on Mount Etna, Stromboli and Vulcano, used a similar approach implemented afterwards on GOES-IMAGER satellite (Harris *et al.,* 1999). Nonetheless, these methodologies do not always remain reliable, mainly because of the chosen fixed threshold approach that prevents their reliability under several observational conditions. In daytime, for example, solar radiation reflected by exposed soils as well as clouds (absorbing the radiation thermally emitted by the Earth surface more in the TIR band 4 of AVHRR, than in the MIR band 3) can produce ΔT_{3-4} greater than 10 K even far, or independently, from any volcanic thermal activity (Marchese, 2001).

Figure 3 (left side) shows two examples of such effects in the case of two eruptive events which occurred at Mount Etna in February 1999 and in July 2001. In the first case (22nd February 1999, 17 GMT, top-left) both the above mentioned effects (due to meteorological clouds and/or exposed soils) are present. In the second one (23rd July 2001, 15 GMT, bottom-left) mainly the volcanic plume, but also high reflective exposed or sparsely vegetated soils, are mistaken for active lava flows.

Also in this case, the RAT approach could permit us to simply overcome the problem of such false detections, increasing, at the same time, (as we will see in the following), the sensitivity toward thermal anomalies of lower intensity.

Starting once more from the general expression (1.1) and considering the variable $V(x, y, t) = T_3(x, y, t)$, a simple ALICE index can be defined as

$$\otimes_{T_3}(x,y,t) = \frac{T_3(x,y,t) - \langle T_3(x,y)\rangle}{\sigma_{T_3}(x,y)} \qquad (3.1)$$

where the quantities $\langle T_3(x, y)\rangle$ and $\sigma_{T_3}(x, y)$ are, respectively, the mean value and the standard deviation of the MIR signal $T_3(x, y, t)$, computed, for each location (x, y), over a long-term series of unperturbed satellite records collected under similar observational conditions. It should be noted that:

i) As $\otimes_{T_3}(x, y, t)$ index gives the excess of the MIR signal, $T_3(x, y, t)$, observed at time t, compared to its «unperturbed» value, historically observed at the same place, (x, y) and under similar observational conditions (*i.e.* same month of the year, same hours of the day, same sensor etc.), false detections due to site effects are expected to be strongly reduced. In fact, surface properties (high reflective exposed soils, warming volcanic rocks, etc.) are expected to be quite similar during the same period of the year (month) and of the day (hours), so low values of $\otimes_{T_3}(x, y, t)$ are expected in these cases, even in the presence of high values of $T_3(x, y, t)$.

ii) Residual fluctuations of the $T_3(x, y, t)$ signal, possibly due to the variability of natural (*e.g.*, atmospheric or surface properties) or observational (*e.g.*, satellite time of pass, navigation and co-location errors, etc.) causes, are all included in the $\sigma_{T_3}(x, y)$ denominator term, which further reduces $\otimes_{T_3}(x, y, t)$ values in the presence of highly variable *llocal* observation conditions.

iii) The use of a single channel approach avoids false detections due to the presence of clouds that, as explained before, mainly originated from the use of a dual-band index.

In the cases of the above mentioned February 1999 and July 2001 events, the $\otimes_{T_3}(x, y, t)$ index was computed following the general prescriptions of the RAT approach (for details see: Tra-

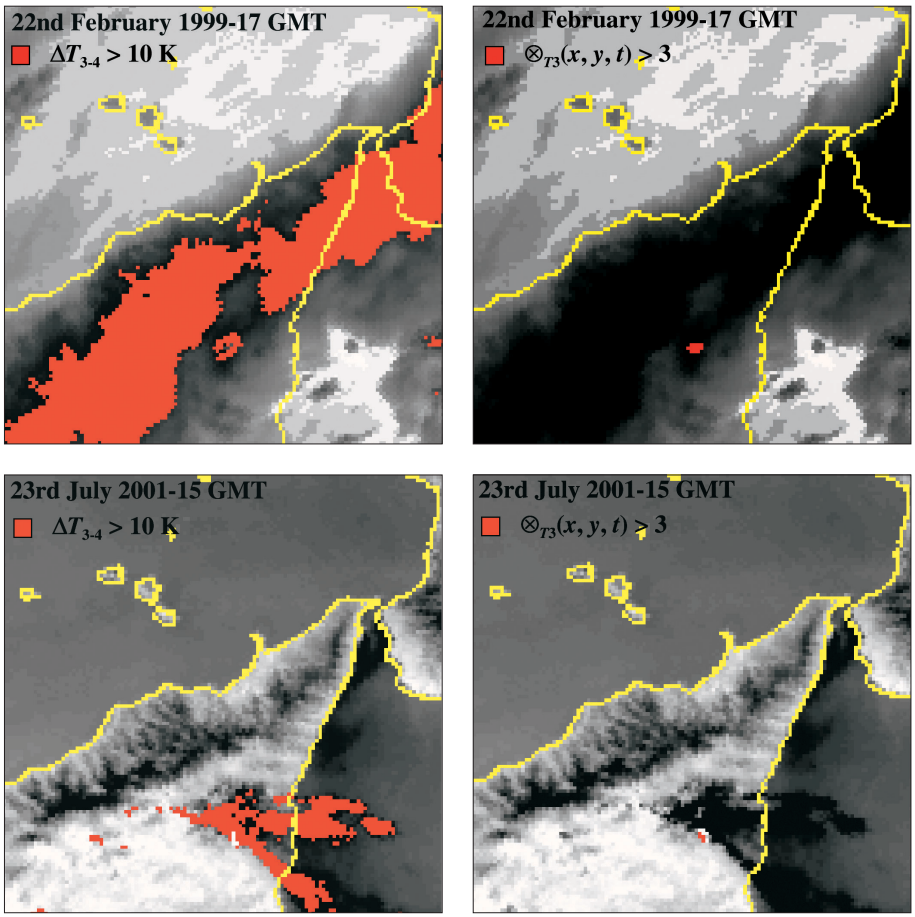

Fig. 3. The NOAA-AVHRR images above show the comparison between (*left*) the fixed threshold method of Harris *et al.* (1995) and the RAT technique (*right*) on February 22nd 1999, 17:00 GMT (*top*) and July 23rd 2001, 15:00 GMT (*bottom*) during Mount Etna eruptive activity: pixels identified as lava flows (see text) are depicted in red. In background AVHRR channel 4 Brightness Temperatures are depicted in grey tones (light tones correspond to lower BT values). Note how on 22nd February 1999 (*top-left*) the fixed threshold method generates several false alarms because of sensitivity of clouds to the dual-band test used. This problem does not affect (*top-right*) the RAT technique (based on a single-band) that detects hot-spots only on Mount Etna according to lava flows produced by the fracture opened on the flanks of volcano starting from 4th February 1999. In the case of 23rd July 2001 (*bottom-left*), the volcanic plume as well as high reflective soils are mistaken for lava flows by the fixed threshold approach. RAT technique (*bottom-right*) recognizes only hot-spots associated with the lava flows effectively produced from a series of new vents opened starting from 17th July.

mutoli, 1998). In the first example (22nd February 1999, 17 GMT), reference images of $\langle T_3 \cdot \cdot (x,\ y)\rangle$ and $\sigma_{T_3}(x,\ y)$ were computed using all the afternoon (17:00-19:00 GMT) NOAA-AVHRR passes on the investigated area acquired during the month of February throughout years 1995-2001.

In the second case (23rd July 2001, 15 GMT), they were computed using all the noon (12:00-15:00 GMT) NOAA-AVHRR passes acquired

during the month of July in the same period (1995-2001). In both cases a *kσ-clipping-filter* (Tramutoli, 1998) was applied to exclude the contribution coming from clouds or hot-spots possibly present in the historical data sets from the computation of the reference fields. In order to reduce further spurious contributions to $\sigma_{T_3} \cdot \cdot (x, y)$, all imagery was precisely navigated using the SANA scheme (Pergola and Tramutoli, 2000) before co-locating them in the same geographic projection.

From the right side of fig. 3, it is possible to infer, also by comparison with the results (shown on the left side) obtained by the dual-band, the fixed threshold approach of Harris *et al.* (1995), the robustness of the $\otimes_{T_3}(x, y, t)$ index against the proliferation of false hot-spot detection. The $\otimes_{T_3} \cdot \cdot (x, y, t)$ index is, in fact, intrinsically not sensitive to reflected solar radiation effects due to soil properties which, under the same observational conditions (month of the year, time of the day, etc.) always occur in a similar way (they are *llocally normal*), producing low values of $\otimes_{T_3}(x, y, t)$ even in the presence of high values of $T_3(x, y, t)$.

In the case of 22nd February 1999, where $\Delta T_{3-4} > 10$ K test mistakes meteorological clouds for hot-spots, the RAT approach detects thermal anomalies only in correspondence with documented Mount Etna lava flows (in this case those produced by the fracture opened on the South East side of the South East Crater on 4th February 1999 that produced abundant lava flows toward Valle del Bove until November 1999: Behnke, 1999).

In the case of 23rd July 2001, where high reflective soils and the whole volcanic plume were mistaken for hot-spots, the RAT technique (right-side) identifies only the thermal anomalies associated with the lava flows produced from a series of new vents opened starting from 17th July (Behnke, 1999).

Together with its robustness against false identification, the proposed approach offers the possibility to evaluate the intensity of anomalous $T_3(x, y, t)$ transients in terms of their normal variability $\sigma_{T_3}(x, y)$. In the previous examples (fig. 3), signal excesses higher than $3\sigma_{T_3}$ (*i.e.* $\sigma_{T_3}(x, y, t) > 3$) were considered, but thermal anomalies of lower (*llocal*) intensity could also be usefully investigated. As an example, fig. 4 reports the result of the hot-spots detection performed by using a 3σ cut (*i.e.* $\otimes_{T_3}(x, y, t) > 3$) on the NOAA-AVHRR image of 13th July 2001. Three thermal anomalies are detected on Mount Etna, in accordance with the strombolian eruptions from the South East and Levantino craters that occurred on 7th and 13th July with emission of lava flows directed toward Valle del Bove (Behnke, 2001). In the same figure, the aforementioned thermal anomalies are also superimposed on a cartographic map of Mount Etna area. In this case, locations with $\otimes_{T_3}(x, y, t) > 2$ are depicted (in yellow) together with the ones with $\otimes_{T_3} \cdot \cdot (x, y, t) > 3$ (in red), in order to investigate spatial distribution of thermal anomalies with different intensity. Thermal anomalies of lower intensity are associated here with smaller portions of AVHRR pixel affected by molten lava, coming from minor (and/or to the borders of the main) lava flows originated as a consequence of the 7th and 13th July Mount Etna eruptions. A single thermal anomaly, that cannot be related to the lava flows from SE Crater and Levantino, is clearly present within the area where, four days later, a new eruptive fracture opened, at an elevation of about 2700 m, throwing out thick lava flows. This fracture was one of the most active and dangerous, and its lava flows threatened Rifugio Sapienza and destroyed part of the cable-car before crossing the Provincial Road SP-92. Even if such analysis was confirmed by direct ground observation (reporting a sudden and intense air warming at the same place and on the same day, S. Longhitano, private comunication), further studies on an extended statistics of eruptive events are obviously required to better assess this result.

Such preliminary results suggest that, thanks to the use of *llocal* thresholds, the proposed approach is not only robust against false hot-spot detections, but also sensitive to signal transients of lower intensity, that (if their relationship with pre-eruptive magma rise is confirmed) could open new possibilities to a better definition of procedures forewarning eruptive events.

4. Seismically active area monitoring

The dependence of AVHRR TIR signal on several natural (*e.g.*, atmospheric transmittance,

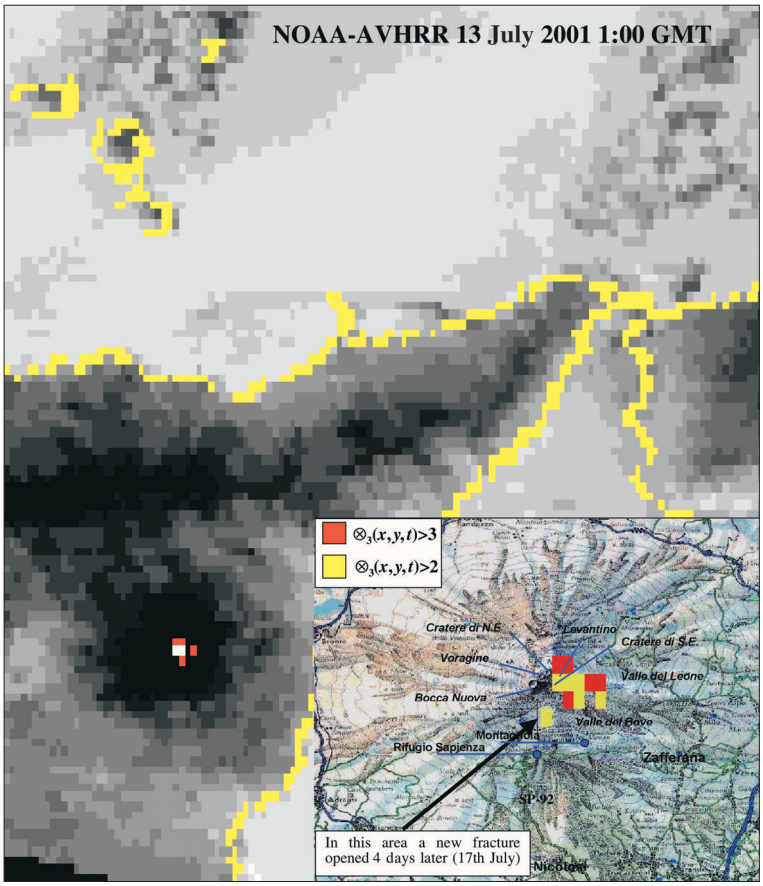

Fig. 4. NOAA/AVHRR July 13th 2001, 1:00 GMT: hot-spots depicted in red are the ones detected by RAT (at $\otimes_3 (x, y, t) > 3$) on Mount Etna in correspondence with lava flows consequent to the strombolian eruptions from SE Crater and Levantino which occurred on 7th and 13th July. In background AVHRR channel 4 brightness temperatures are depicted in grey tones (light tones correspond to lower BT values), coast-lines are depicted in yellow. Results of RAT analysis are projected on a map of Mount Etna shown in the box corner. In this case also thermal anomalies of lower intensity (with $\otimes_3 (x, y, t) > 2$) are depicted (in yellow). Note the isolated anomaly (that, differently from the others, cannot be related to lava flows) detected within the area where four days later a new eruptive fracture opened, throwing out lava flows (see text).

surface temperature, spectral emissivity and topography) and observational (time/season, but also satellite view angles) conditions has been stressed in a recent study (Tramutoli *et al.*, 2001b) of the Irpinia-Basilicata earthquake (November 23rd, 1980, $M_S = 6.9$).

In that case, the considered variable was the difference $V(x, y, t) = T_4(x, y, t) - T_4(t) \equiv \Delta T_4 \cdot (x, y, t)$ between the current signal $T_4(x, y, t)$ (TIR radiance in the AVHRR channel 4) measured at location (x, y) and its spatial average $T_4(t)$ computed in place, on the image at hand, considering all cloud-free pixels belonging to the same, land or sea, class. According to the general expression (1.1), the corresponding ALICE index was

$$\otimes_{\Delta T_4}(x,y,t) = \frac{\Delta T_4(x,y,t) - \langle \Delta T_4(x,y) \rangle}{\sigma_{\Delta T_4}(x,y)} \quad (4.1)$$

where quantities $\langle \Delta T_4 (x, y) \rangle$ and $\sigma_{\Delta T_4} (x, y)$ are, respectively, the mean value and the standard deviation of the differential signal $\Delta T_4 (x, y, t)$ computed, for each location (x, y), over a long-term series of unperturbed satellite records collected under similar observational conditions. It should be noted that, also in this case:

i) As $\otimes_{\Delta T_4} (x, y, t)$ index gives the excess of $\Delta T_4 (x, y, t)$ signal, observed at time t compared to its «unperturbed» value, historically observed at the same place, (x, y) and under similar observational conditions (*i.e.* same month of the year, same hours of the day, same sensor, etc.), false anomalies due to site effects (*e.g.*, land cover, altitude, etc.) are expected to be strongly reduced. In fact, altitude can be assumed constant (for the same location) and other important surface properties, like emissivity and temperature, are expected to be quite similar during the same period of the year (month) and day (hours). Low values of $\otimes_{\Delta T_4} (x, y, t)$ are then expected even in the presence of high values of $\Delta T_4 (x, y, t)$ and a flat spatial distribution of $\otimes_{\Delta T_4} (x, y, t)$ even in presence of a high spatial variability of $\Delta T_4 (x, y, t)$ signal (see for instance: Tramutoli *et al.* (2001b) where the independence of $\otimes_{\Delta T_4} (x, y, t)$ index from altitude is demonstrated in the case of a highly variable orography)!

ii) The choice of a differential variable $\Delta T_4 \cdot (x, y, t)$, instead of $T_4 (x, y, t)$, is expected to reduce a possible contribution (*e.g.*, occasional warming) to the signal due to year-to-year climatological changes and/or season time-drifts. In fact, such effects are expected to affect both $T_4 (x, y, t)$ and $T_4 (t)$ terms of $\Delta T_4 (x, y, t)$ in a similar way.

iii) Residual fluctuations of the $\Delta T_4 (x, y, t)$ signal, possibly due to the variability of natural (mainly atmospheric water vapour content) or observational (*e.g.*, satellite time of pass, navigation and co-location errors, etc.) causes, are all included in the $\sigma_{\Delta T_4} (x, y)$ denominator term which further reduces $\otimes_{\Delta T_4} (x, y, t)$ values in the presence of highly variable *llocal* observation conditions.

In the quoted study (Tramutoli *et al.*, 2001b) on the Irpinia-Basilicata earthquake (November 23rd, 1980, $M_S = 6.9$), five years (1994-1998) of NOAA-AVHRR images (acquired during the month of November around 18:00 GMT) were used to compute the reference images of $\langle \Delta T_4 \cdot (x, y) \rangle$ and $\sigma_{\Delta T_4} (x, y)$. The $\otimes_{\Delta T_4} (x, y, t)$ index was then computed for the month of November 1980 (validation) as well as for other, seismically unperturbed (no seismic events with $M_S > 4$ in the investigated area/period) years (falsification). Even if higher values of $\otimes_{\Delta T_4} (x, y, t)$ (almost absent in the «unperturbed» years considered) were found in some correlation with the spatial distribution of seismogenic areas and with time of earthquake occurrence, they rarely reached values greater than 0.6. This means that the observed signal was still deep in the natural/observational noise accounted by very high $\sigma_{\Delta T_4} (x, y)$ values. The main contributions to the high *llocal* variability of the $\Delta T_4 (x, y, t)$ signal were identified in the high space-time dynamics of atmospheric water vapour content as well as in the variability of satellite view angles (characteristic of polar satellites like NOAA and differently from geo-stationary platforms).

In fact, water vapour is one of the most variable components of the atmosphere, partly absorbing the outgoing, Earth-emitted TIR radiation. Variations of atmospheric water vapour content contribute to further increase *llocal* variability of the measured $\Delta T_4 (x, y, t)$ signal. Moreover, even if AVHRR images are precisely navigated and co-located (in order to permit the computation of reference images $\langle \Delta T_4 (x, y, t) \rangle$ and $\sigma_{\Delta T_4} (x, y)$ by a multi-temporal analysis), at each revisiting time t the same location (x, y) is observed at different satellite zenithal angles (which also means different ground-resolution cells). This circumstance may produce a further spurious temporal variation of the measured signal. It should be noted, however, that all the residual «noisy» contributions to the TIR signal (including the above mentioned ones related to the variability of atmospheric conditions and view angles) are intrinsically taken into account by the RAT approach, as they generally increase the *llocal* value of $\sigma_{\Delta T_4} (x, y)$ reducing corresponding $\otimes_{\Delta T_4} (x, y, t)$ values and, consequently, false anomaly appearance probability.

In order to take into account the effects related to atmospheric water vapour variability, we applied a different ALICE index to the same event (Irpinia-Basilicata earthquake) using the same AVHRR data-set (November 1994-1998, 18:00 GMT)

$$\otimes_{\Delta\mathrm{LST}}(x,y,t) = \frac{\Delta\mathrm{LST}(x,y,t) - \langle\Delta\mathrm{LST}(x,y)\rangle}{\sigma_{\Delta\mathrm{LST}}(x,y)}. \tag{4.2}$$

It differs from the one defined in expression (4.1) due to the use, instead of the simple TIR signal $T_4\,(x,\,y,\,t)$, of the LST (Land Surface Temperature) AVHRR product, obtained following the Becker and Li (1990) split-window technique

$$\begin{aligned}\mathrm{LST} &= 1.274 + \frac{T_4+T_5}{2}\cdot\\ &\cdot\left[1+\left(0.15616\cdot\frac{1-\varepsilon}{\varepsilon}\right)-\left(0.482\cdot\frac{\Delta\varepsilon}{\varepsilon^2}\right)\right]+\\ &+\frac{T_4-T_5}{2}\left[6.26+\left(3.98\cdot\frac{1-\varepsilon}{\varepsilon}\right)+\left(38.33\cdot\frac{\Delta\varepsilon}{\varepsilon^2}\right)\right].\end{aligned} \tag{4.3}$$

Here, ε_4 and ε_5 are, respectively, the emissivity in the AVHRR channel 4 and 5, $\Delta\varepsilon = (\varepsilon_4 - \varepsilon_5)$ and $\varepsilon = (\varepsilon_4 + \varepsilon_5)/2$, T_4 and T_5 the radiances (expressed in brightness temperature) measured in AVHRR TIR channel 4 (around 11 μm) and 5 (around 12 μm). The algorithm mainly exploits the direct proportionality expected between atmospheric Total Water Vapour Content (TWVC) and the measured difference $T_4 - T_5$ (due to the higher extinction operated by atmospheric water vapour in the AVHRR channel 5 than in channel 4) to correct land surface temperature estimates for the effect of atmospheric water vapour content. Using the values ($\varepsilon_4 = 0.95$ and $\varepsilon_5 = 0.96$) suggested by Becker and Li for the month of November, expression (4.3) reduces to

$$\begin{aligned}\mathrm{LST}(x,y,t) &= 1.274 +\\ &+\frac{1.01264\cdot\left[T_4(x,y,t)+T_5(x,y,t)\right]}{2}+\\ &+\frac{6.027\cdot\left[T_4(x,y,t)-T_5(x,y,t)\right]}{2}\end{aligned} \tag{4.4}$$

that well emphasizes how such algorithm basically exploits only T_4 and T_5 AVHRR radiances.

Even if the comparison with ground based observations ascribes quite high biases to such LST estimates (> 3°C rms, Pozo Vasquez *et al.*, 1995), the correlation with near-surface thermal conditions has been demonstrated to be quite high (more than 95%, Cuomo *et al.,* 2002) in the temporal domain. Such biases on LST estimates, as well as the parametric choice of surface emissivity values (based only on the season and not on local surface properties) are both expected not to affect the $\otimes_{\Delta\mathrm{LST}}$ index that is in fact based on LST variations (both in space and time domains) and not on its absolute values.

Figure 5 summarizes the result of the analysis performed in the case of the strong earthquake ($M = 6.9$) which occurred in Southern Italy (Irpinia-Basilicata) on November 23, 1980 at 7.32 p.m. local time. This is the same event already analysed in a previous study (Tramutoli *et al.*, 2001b) by using the $\otimes_{\Delta T}$ index instead of $\otimes_{\Delta\mathrm{LST}}$. As in that study, also in this case all NOAA/AVHRR satellite passes, collected in November from 1994 to 1998 around 18:00 GMT over the Southern Italian peninsula, were processed in order to build the average, $\{\Delta\mathrm{LST}(x,y)\}$ and standard deviation $\sigma_{\Delta\mathrm{LST}}\,(x,\,y)$, reference images. In the same way, monthly averages $\otimes_{\Delta\mathrm{LST}}\,(x,\,y)$ of $\otimes_{\Delta\mathrm{LST}}\,(x,\,y,\,t)$ were computed for the month of November 1980 (the year of the earthquake for validation purposes) and for the relatively unperturbed (no earthquakes with $M_S > 4$) years 1994 and 1998 (for falsification purposes). The results of this analysis are reported in fig. 5, where pixels with $\otimes_{\Delta\mathrm{LST}}\,(x,\,y) > 1$ are depicted in red and aftershock locations in green. By comparison with results previously achieved by using the $\otimes_{\Delta T}$ index (see Tramutoli *et al.*, 2001b) it is possible to note that:

i) For November 1980 (validation), the spatial distribution of pixels with $\otimes_{\Delta\mathrm{LST}}\,(x,\,y) > 1$ is quite similar to the one of pixel with $\otimes_{\Delta T_4} > 0.6$.

ii) As far as unperturbed years (November 1994 and 1998) are concerned (falsification), pixels with $\otimes_{\Delta\mathrm{LST}}\,(x,\,y) > 1$ almost disappear with respect to the already rare presence of pixels with $\otimes_{\Delta T_4} > 0.6$.

It seems that the use of the $\otimes_{\Delta\mathrm{LST}}$ index, instead of $\otimes_{\Delta T_4}$ (*i.e.* taking into account the

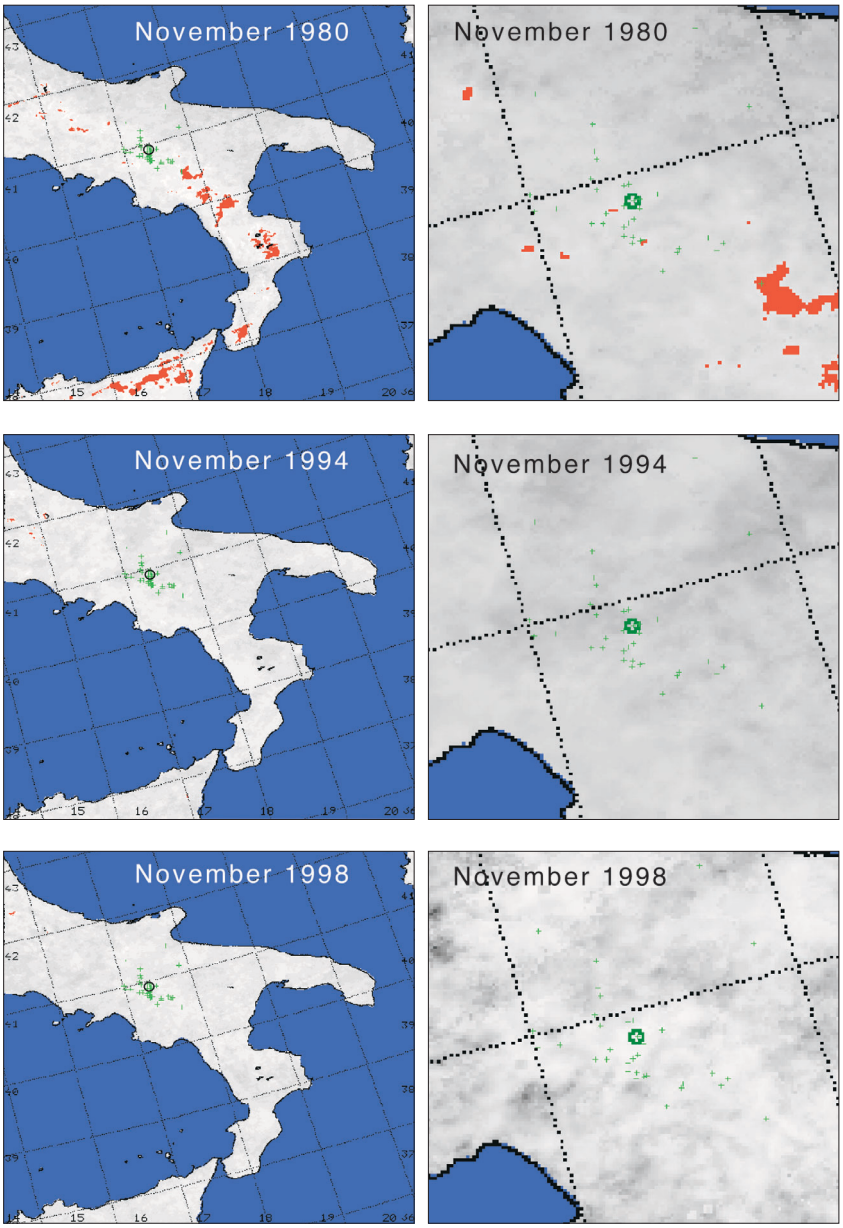

Fig. 5. Results of the analysis on monthly averages $\otimes_{\Delta LST}(x, y)$ of $\otimes_{\Delta LST}(x, y, t)$ index (computed on the basis of NOAA-AVHRR images collected around 18:00 GMT during the months of November from 1994 and 1998) for the month of November 1980, 1994 and 1998 (see text). The aftershocks of the Irpinia-Basilicata earthquake (November, 23th, 1980, $M = 6.9$) and the main epicentral area (circled) are depicted in green. Pixels with $\otimes_{\Delta LST}(x, y) > 1$ are depicted in red. The zooms, on the epicentral area, of images shown on the left are shown on the right side. Note the absence of high $\otimes_{\Delta LST}(x, y)$ values in the unperturbed (no earthquakes with $M > 4$) month of November 1994 and 1998.

contribution to TIR signal variability due to variations of the atmospheric water vapour content) mainly produces a reduction of the *llocal* value of $\sigma_{\Delta LST}(x, y)$, (compared to $\sigma_{\Delta T_4} \cdot \cdot (x, y)$), permitting a substantial increase in the Signal-to-Noise (S/N) ratio (inherent in the definition of ALICE indexes) from 0.6 to 1.

Also the indications (*e.g.,* on the possible relations between occurrence of higher $\otimes_{\Delta T_4}$ values and seismogenic area distribution and activation) from the previous study of Tramutoli *et al.* (2001b) appear reinforced by the increased S/N ratio associated with the observed $\otimes_{\Delta LST}$ space-time patterns. Their confirmed extension, far away (up to several hundred kilometres) from the epicentral zone is of no minor importance, reinforcing the idea that spatial resolution is not the main constraint for satellite packages devoted to such studies.

Further reductions of the observational noise can then be expected by the extension of the proposed technique to geo-stationary satellites, like Meteosat. In particular, significant improvements are to be expected by the extension of the proposed approach to MSG-SEVIRI (Meteosat Second Generation-Spinning Enhanced Visible and Infra-Red Imager) offering a time resolution of 15 min and a channel selection that saves (and extends) present AVHRR capabilities.

Even at a lower spatial resolution (3 km compared with 1.1 km of AVHRR in the TIR channels) and thanks to the MSG geo-stationary attitude, SEVIRI will offer:

i) A precise navigation and image-to-image co-location, as well as constant (for each location) view-angles that permit a significant reduction of the observational noise and an increase in the sensitivity of the proposed method, which strongly relies on the multi-temporal analysis of satellite radiance at pixel level.

ii) An improved time-resolution that will reduce both the natural (lower image-to image variability of the *llocal* signal) and observational (greater homogeneity of time-series elements) noise, increasing once more the sensitivity of ALICE indices toward relatively lower signal variations.

5. Summary and discussion

Most of the satellite techniques proposed to date for seismic and volcanic activity monitoring, make use of a «fixed threshold» approach that, due to the space-time variability of Earth surface (and atmospheric) conditions, often produces missing or false detections of investigated phenomena. These techniques, in fact, do not allow for all those factors, not related to the event under study, whose variable contribution to the measured signal can completely mask (or simulate) the effects of the event to be investigated. A different, self-adaptive, approach (RAT) has recently been proposed (Tramutoli, 1998) which permits us to recognize (by comparison with a *normal* signal behavior automatically defined at the pixel level on the basis of the site-history) space-time signal transients, also in the presence of highly variable contributions from atmospheric (*e.g.*, water vapor content), surface (*e.g.,* emissivity) and observational (time/season, view angles) conditions.

In this paper, the theoretical basis for the extension of RAT approach to several aspects of volcanic and seismic activity monitoring has been presented.

Volcanic ash-cloud detection during daytime was already treated by a similar approach (Pergola *et al.*, 2001) using AVHRR bands falling in the SOR (solar reflected) spectral region. In this work, a RAT approach based on TIR and MIR AVHRR bands has been proposed which extends such a possibility to night time. A RAT approach, similar to the one already used (Cuomo *et al.*, 2001) for wildfire detection, has been proposed for lava flow (which exhibits similarly high radiant temperature in the MIR spectral region) detection and to investigate possible pre-eruptive thermal anomalies.

The problem of seismic area monitoring by satellite TIR surveys was already treated (Tramutoli *et al.*, 2001b) applying the RAT approach to the Irpinia-Basilicata earthquake ($M_S = 6.9$) which occurred on November 23, 1980 in Southern Italy. In this paper, a substantial S/N increase (from 0.6 to 1.0) has been achieved, allowing for the dependence of measured TIR signal on atmospheric water vapour content variability.

For all the considered topics, the proposed approach seems to confirm its robustness against false detections (especially important for operational monitoring purposes) and its sensitivity toward signal transients of lower intensity. Its intrinsic exportability (only satellite data are required), not only in different geographic areas but also on different satellite instrumental packages is no minor merit. In particular, benefits expected by its extension to present and incoming geo-stationary satellite packages have been particularly stressed for application to seismically active area monitoring by TIR surveys.

Acknowledgements

This work was carried out within the framework of SEISMASS (contract No. I/R/173/02) and FASA (contract No. I/R/203/02) projects funded by ASI (Agenzia Spaziale Italiana).

REFERENCES

BECKER, F., and Z.L. LI (1990): Toward a local split window over land surfaces**,** *Int. J. Remote Sensing*, **11** (3), 369-393.

BEHNKE, B. (1999): Italy's volcanoes, in *The Cradle of Volcanology* (on line: http://www.geo.mtu.edu./~boris/ETNA.html).

BEHNKE, B. (2001): Italy's volcanoes, in *The Cradle of Volcanology* (on line: http://www.geo.mtu.edu./~boris/ETNA.html).

CARN, S.A. and C. OPPENHEIMER (2000): Remote monitoring of Indonesia Volcanoes using satellite data from the Internet, *Int. J. Remote Sensing*, **21** (5), 873-910.

CUOMO, V., R. LASAPONARA and V. TRAMUTOLI (2001): Evaluation of a new satellite-based method for forest fire detection, *Int. J. Remote Sensing*, **22** (9), 1799-1826.

CUOMO, V., N. AFFLITTO, M. BLUMETTI, A. BONFIGLIO, O. CANDELA, T. CARONE, G. DI BELLO, C. FILIZZOLA, T. LACAVA, A. LANORTE, V. LANORTE, R. LASAPONARA, M. MACCHIATO, L. MINERVINI, F. MUNDO, N. PERGOLA, C. PIETRAPERTOSA, S. PIGNATTI, F. ROMANO, T. SIMONIELLO, V. TRAMUTOLI and A. ZACCAGNINO (2002): Pollino Project Action D: a multi-scale approach, in the space-time domain, to environmental risk monitorino, in *Remote Sensing for Environmental Monitoring, GIS Applications and Geology*, edited by M. EHLERS, *Proc. SPIE*, **4545**, 13-23.

DAVIES, M.A. and W.I. ROSE (1998): GOES imagery fills gaps in Montserrat volcanic cloud observations, *Eos*, **79**, 505-507.

ELLROD, G.P. and B.H. CONNEL (1999): Improvements in volcanic ash detection using GOES multispectral image data, in *Conference on Aviation, Range, and Aerospace Meteorology*, **8**, 326-329.

GAWARECKI, S.J., R.J.P. LYON and W. NORDBERG (1965): Infrared spectral returns and imagery of the Earth from space and their application to geological problems, *Am. Astron. Soc., Sci. Technol. Ser.*, **4**, 13-33.

GORNY, V.I., A.G. SALMAN, A.A. TRONIN and B.B. SHILIN, (1988): The Earth outgoing IR radiation as an indicator of seismic activity, *Proc. Acad. Sci. USSR*, **301**, 67-69.

HARRIS, A.J. and S.E.J. SWABEY (1995): Automated threshold of active lava using AVHRR data, *Int. J. Remote Sensing*, **16** (18), 3681-3686.

HARRIS, A.J., L.R.A. VAUGHAN and D.A. ROTHERY (1995): Volcano detection and monitoring using AVHRR data: the Krafla eruption, 1984, *Int. J. Remote Sensing*, **16**, 1001-1020.

HARRIS, A.J.L., R. WRIGHT and L.P. FLINN (1999): Remote monitoring of Mount Erebus volcano, Antarctica, using polar orbiters: progress and prospect, *Int. J. Remote Sensing*, **20** (15-16), 3051-3071.

HIGGINS, J. and A.J.L. HARRIS (1997): Vast: a program to locate and analyse volcanic thermal anomalies automatically from remotely sensed data, *Comput. Geosci.*, **23** (6), 627-645.

HOLASEK, R.E. and W.I. ROSE (1991): Anatomy of 1986 Augustine volcano eruptions as recorded by multispectral image processing of digital AVHRR weather satellite data, *Bull. Volcanol.*, **53**, 420-435.

KROTKOV, N.A., O. TORRES, C. SEFTOR, A.J. KRUEGER, A. KOSTINSKI, W.I. ROSE, G.J.S. BLUTH, D. SCHNEIDER and S.J. SCHAEFER (1999): Comparison of TOMS and AVHRR Volcanic Ash retrievals from the August 1992 Eruption of Mt. Spurr, *Geophys. Res. Lett.*, **26** (4), 455-458.

MARCHESE, F. (2001): Tecniche satellitari avanzate per il monitoraggio dell'attività vulcanica nell'infrarosso termico, *D.Thesis* (University of Basilicata, Potenza, Italy).

OPPENHEIMER, C. (1998): Volcanological applications of meteorological satellites, *Int. J. Remote Sensing*, **19** (15), 2829-2864.

PERGOLA, N. and V. TRAMUTOLI (2000): SANA: Sub-pixel Automatic Navigation of AVHRR imagery, *Int. J. Remote Sensing Lett.*, **21** (12), 2519-2524.

PERGOLA, N., C. PIETRAPERTOSA, T. LACAVA and V. TRAMUTOLI (2001): Robust satellite techniques for monitoring volcanic eruptions, *Ann. Geophysics*, **44** (2), 167-177.

PIETRAPERTOSA, C., N. PERGOLA, V. LANORTE and V. TRAMUTOLI (2001): Self adaptive algorithms for change detection: OCA (the One-channel Cloud-detection Approach) an adjustable method for cloudy and clear radiances detection, in *Technical Proceedings of the 11th International (A)TOVS Study Conference (ITSC-XI),* Budapest, Hungary, 20-26 September 2000, edited by J.F. LE MARSHALL and J.D. JASPER (Bur. Meteorol. Res. Centre, Melbourne, Australia), 281-291.

POZO VASQUEZ, D., F.J. OLMO REYES and L. ALADOS ARBOLEDAS (1995): A comparison of land surface temperature algorithms, in *The Meteorological Satellite Data Users' Conference, Polar Systems*, *EUMETSAT* (Germany), 223-230.

PRATA, A.J. (1989): Observations of volcanic ash clouds in the 10-12 μm window using AVHRR/2 data, *Int. J. Re-*

mote Sensing, **10**, 751-761.

QIANG, Z. and D. CHANG-GONG (1992): Satellite thermal infrared impending temperature increase precursor of Gonghe earthquake of magnitude 7.0, Qinghai Province, *Geoscience*, **6** (3), 297-300.

QIANG, Z., X. XIU-DENG and D. CHANG-GONG (1997): Thermal infrared anomaly – Precursor of impending earthquakes, *Pure Appl. Geophys.*, **149**, 159-171.

ROSE, W.I. and D.J. SCHNEIDER (1996): Satellite images offer aircraft protection from volcanic ash clouds, *Eos, Trans. Am. Geophys. Un.*, **77**, 529-530.

SCAFFIDI, I.G. (2001): Tecniche satellitari robuste per il monitoraggio delle nubi vulcaniche, *D.Thesis* (University of Basilicata, Potenza, Italy).

SCHNEIDER, D.J. and W.I. ROSE (1994): Observations of the 1989-90 Redoubt Volcano eruption clouds using AVHRR satellite imagery, in *Proceedings of the First International Symposium on Volcanic Ash and Aviation Safety*, edited by T. CASADEVALL, *U.S. Geol. Surv. Bull.,* **2047**, 405-418.

SCHNEIDER, D.J. and W.I. ROSE (1995): Tracking of the 1992 Crater Peak/Spurr eruption clouds using AVHRR, *U.S. Geol. Surv. Bull.*, **2139**, 27-36.

SEFTOR, C.J, N.C. HSU, J.R. HERMAN, P.K. BHARTIA, O. TORRES, W.I. ROSE, D.J. SCHNEIDER and N. KROTKOV (1997): Detection of volcanic ash clouds from Nimbus/7 total ozone mapping spectrometer, *J. Geophys. Res.*, **102** (D14), 16749-16759.

SIMPSON, J.J., G. HUFFORD, D. PIERI and J. BERG (2000): Failures in detecting volcanic ash from a satellite-based technique, *Remote Sensing Environ.*, **72**, 191-217.

TRAMUTOLI, V. (1998): Robust AVHRR Techniques (RAT) for environmental monitoring: theory and applications, in *Earth Surface Remote Sensing II*, edited by G. CECCHI and E. ZILIOLI, *Proc. SPIE*, **3496**, 101-113.

TRAMUTOLI, V., N. PERGOLA and C. PIETRAPERTOSA (2001a): Training on NOAA-AVHRR of robust satellite techniques for next generation of weather satellites: an application to the study of space-time evolution of Pinatubo's stratospheric volcanic cloud over Europe, in *IRS 2000: Current Problems in Atmospheric Radiation,* edited by W.L. SMITH and YU.M. TIMOFEYEV (A. Deepak Publishing, Hampton, Virginia), 36-39.

TRAMUTOLI, V., G. DI BELLO, N. PERGOLA and S. PISCITELLI (2001b): Robust satellite techniques for remote sensing of seismically active areas, *Ann. Geophysics*, **44** (2), 295-312.

TRONIN, A.A. (1996): Satellite thermal survey – a new tool for the study of seismoactive regions, *Int. J. Remote Sensing*, **17** (8), 1439-1455.

TRONIN, A.A., M. HAYAKAWA and O.A. MOLCHANOV (2002): Thermal IR satellite data application for earthquake research in Japan and China, *J. Geodyn.*, **33** (4-5), 519-534.

WEN, S. and W.I. ROSE (1994): Retrieval of sizes and total masses of particles in volcanic clouds using AVHRR bands 4 and 5, *J. Geophys. Res.*, **99**, 5421-5431.